PERGAMON

International Journal of Solids and Structures 39 (2002) 5081–5099

INTERNATIONAL JOURNAL OF SOLIDS and STRUCTURES

www.elsevier.com/locate/ijsolstr

A three-dimensional nonlinear model for dissipative response of soft tissue

M.B. Rubin *, S.R. Bodner

Faculty of Mechanical Engineering, Technion—Israel Institute of Technology, 32000 Haifa, Israel

Received 9 June 2001; received in revised form 27 February 2002

Abstract

A set of three-dimensional constitutive equations is proposed for modeling the nonlinear dissipative response of soft tissue. These constitutive equations are phenomenological in nature and they model a number of physical features that have been observed in soft tissue. The equations model the tissue as a composite of a purely elastic component and a dissipative component, both of which experience the same total dilatation and distortion. The stress response of the purely elastic component depends on dilatation, distortion and the stretch of material fibers, whereas the stress response of the dissipative component depends on distortional deformation only. The equations are hyperelastic in the sense that the stress is obtained by derivatives of a strain energy function, and they are properly invariant under superposed rigid body motions. In contrast with standard viscoelastic models of tissues, the proposed constitutive model includes the total deformation rate in evolution equations that can reproduce the observed physical feature that the hysteresis loops of most biological soft tissues are nearly independent of strain rate (Biomechanics, Mechanical Properties of Living Tissues, second ed. (1993)). Material constants are determined which produce good agreement with uniaxial stress experiments on superficial musculoaponeurotic system and facial skin.

Keywords: Biomechanics; Finite deformation; Soft tissue; Viscoelastic; Viscoplastic

1. Introduction

Understanding the response of living tissues to mechanical loads is essential to a wide range of problems that include the design of prosthetic devices and the evaluation of optimal surgical and suturing procedures. This field of study has received considerable attention over the last few decades and much of the research has been reviewed in the book on biomechanics by Fung (1993).

Living tissue is a complicated composite structure that is composed of a number of materials. For example, superficial musculoaponeurotic system (SMAS) and facial skin both contain elastin, collagen, fat cells and water. Moreover, many biological tissues are porous and allow blood flow to supply nutrients to the cells that form the building blocks of the tissue. Biochemical processes, osmotic pressure, growth of

* Corresponding author. Fax: +972-4-832-4533.
E-mail address: mbrubin@tx.technion.ac.il (M.B. Rubin).

0020-7683/02/$ - see front matter © 2002 Published by Elsevier Science Ltd.
PII: S0020-7683(02)00237-8

cells, aging, and environmental factors all contribute to the complicated response of tissue. Also, the material behavior is nonlinear, time dependent and anisotropic.

From a fundamental point of view, it is desirable to develop mathematical models which include all of the important physical processes that are active in living tissues. Specific attempts to model the nonlinear deformations and fluid flow processes in porous media can be found in Vankan et al. (1997) and Huyghe and Janssen (1999).

Such fundamental approaches usually lead to complicated nonlinear partial differential equations. Consequently, attempts to simplify these models by using phenomenological constitutive equations are desirable and can provide sufficient descriptions of the material response for many applications. For example, cardiac muscle has been modeled (Choung and Fung, 1986; Humphrey and Yin, 1987; Horowitz et al., 1988; Humphrey et al., 1990) using phenomenological constitutive equations which include nonlinear elasticity, viscoelasticity and anisotropy due to the response of oriented fibers. Also, the general modeling of soft tissue has been discussed recently by Holzapfel (2001).

Har-Shai et al. (1996) performed mechanical uniaxial stress tests on recently excised strips of facial tissue which included cycles of loading, unloading, reloading at various strain rates, and stress relaxation. These experimental results were modeled by Rubin et al. (1998), and the experimental data are shown in Fig. 1 for SMAS and in Fig. 2 for facial skin (note that the predictions shown in these figures are based on the new model presented below). In these figures Π_{11} is the engineering axial stress (force per unit reference area) and ε_{11} is the engineering axial strain (change in length per unit reference length), both of which were measured in the experiments. Figs. 1(a) and 2(a) show three cycles of loading with the magnitude of the strain rate $\dot{\varepsilon}_{11}$ for cycle 1 being greater than that for cycle 2, which is greater than that for cycle 3. The relaxation tests shown in Fig. 1(b) were performed on a different sample of SMAS than that used in the cyclic loadings of Fig. 1(a), whereas the relaxation tests shown in Fig. 2(b) were performed on the same sample of facial skin used in the cyclic loadings of Fig. 2(a), with the relaxation tests being performed after the cyclic loading tests. Moreover, it will be shown later in Fig. 6 that the differences between the responses to these cycles of loading are due to changes in the internal structure (internal state variables) of the material and not due to the differences in the imposed strain rates.

These figures exhibit material response that seems to be representative of many soft tissues. Specifically, Fung (1993, p. 262) identifies the following physical features

(P1) a nonlinear stress–strain relationship,
(P2) a hysteresis loop in cyclic loading and unloading,

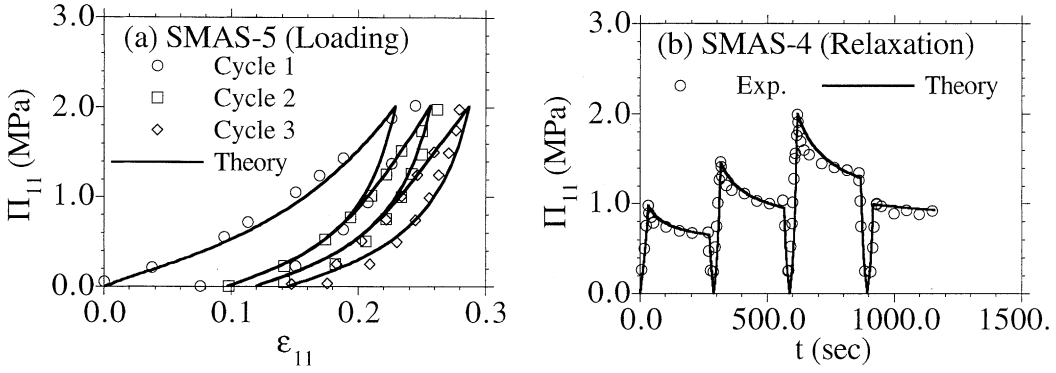

Fig. 1. Response of SMAS: (a) loading and unloading cycles (cycle 1: $\dot{\varepsilon}_{11} = \pm 2.0 \times 10^{-2}$ s^{-1}; cycle 2: $\dot{\varepsilon}_{11} = \pm 5.0 \times 10^{-3}$ s^{-1}; cycle 3: $\dot{\varepsilon}_{11} = \pm 1.0 \times 10^{-3}$ s^{-1}); and (b) stress relaxation cycles ($\dot{\varepsilon}_{11} = \pm 5.0 \times 10^{-3}$ s^{-1} for loading and unloading).

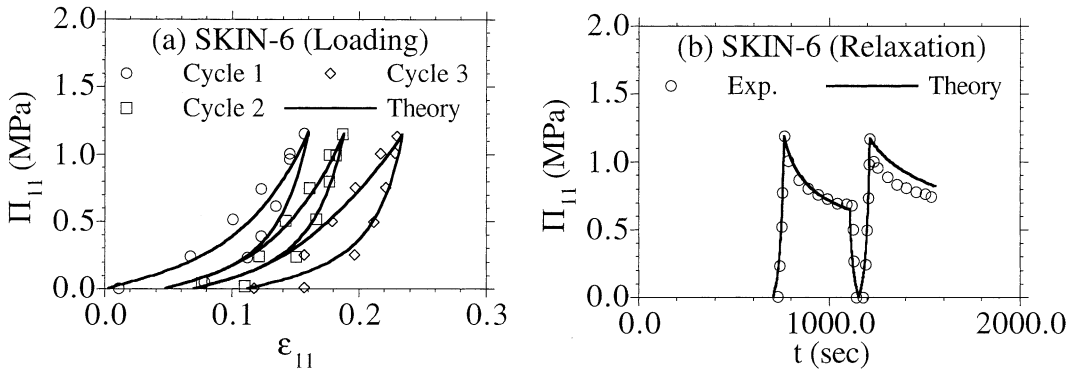

Fig. 2. Response of facial skin: (a) loading and unloading cycles (cycle 1: $\dot{\varepsilon}_{11} = \pm 1.0 \times 10^{-2}$ s^{-1}; cycle 2: $\dot{\varepsilon}_{11} = \pm 2.5 \times 10^{-3}$ s^{-1}; cycle 3: $\dot{\varepsilon}_{11} = \pm 5.0 \times 10^{-4}$ s^{-1}); and (b) stress relaxation cycles ($\dot{\varepsilon}_{11} = \pm 2.5 \times 10^{-3}$ s^{-1} for loading and unloading).

(P3) stress relaxation at constant strain,
(P4) preconditioning in repeated cycles (a tendency to approach a stable cycle, which is associated primarily with elastic response).

The preconditioning phenomena is somewhat apparent in Fig. 1(a) where cycling between fixed stress levels causes the hysteresis loops to reduce in width. This indicates that the material response becomes more elastic. Furthermore, with regard to preconditioning, Fung (1993, p. 262) states that:

> The reason that preconditioning occurs in a specimen is that the internal structure of the tissue changes with the cycling. By repeated cycling, eventually a steady state is reached at which no further change will occur unless the cycling routine is changed. Changing the upper and lower limits of the cycling will change the internal structure again, and the specimen must be preconditioned anew.

Moreover, the additional physical feature

(P5) stress relaxation from a given stress level reduces consequent to repeated cycling,

can be observed from Figs. 1(b) and 2(b).

In addition to the characteristics (P1)–(P5), observations on soft tissues indicate that hysteresis loops to the same stress levels are nearly independent of strain rate over a wide range of rates (Fung, 1993, p. 281). This feature can be stated as an additional property

(P6) the hysteresis loops are nearly independent of strain rate.

The main objective of this paper is to focus attention on modeling the dissipative response of soft tissue. As previously mentioned, detailed modeling of the physical processes that occur in composite structures like soft tissue is quite complicated. Consequently, here attention will be focused on phenomenological constitutive equations.

With a viscoelastic approach (e.g. Neubert, 1963; Puso and Weiss, 1998; Pioletti and Rakotomanana, 2000), hereditary integrals are introduced to account for the effects of the loading history. These integrals are usually represented in terms of a finite number of relaxation times so they cannot predict the physical response (P6). An alternative model for the time-dependent response of tissues, motivated by the unified

constitutive equations for elastic-viscoplastic materials proposed by Bodner and Partom (1975), and Bodner (1987), has been developed by Rubin et al. (1998). Instead of using hereditary integrals, this model uses history dependent state-variables which are determined by evolution equations for their time rates of change.

More specifically, the work of Rubin et al. (1998) developed one-dimensional constitutive equations which modeled all of the physical features (P1)–(P6) and matched the experimental data of Har-Shai et al. (1996) fairly well. The model developed here also models these physical features but it improves on that previous model in three main respects:

(1) it is a full three-dimensional model,
(2) it includes anisotropic effects of material fiber orientations,
(3) it includes elastic components and recovery of hardening (which models recovery of fluid in the unloaded cells) that lead to full recovery of the unloaded shape over time.

An outline of the contents of this paper is as follows: Section 2 provides a discussion of the previous model (Rubin et al., 1998), Section 3 describes the general constitutive equations and Section 4 proposes specific functional forms for the strain energy and the evolution equations. Section 5 describes examples of uniaxial stress and shows that the proposed equations can predict good agreement with experiments on SMAS and facial skin. Section 6 presents conclusions and Appendix A briefly describes aspects of appropriate numerical integration procedures.

Also, throughout the text, $\mathbf{a}\cdot\mathbf{b}$ denotes the dot product between two vectors $\mathbf{a}$ and $\mathbf{b}$; $\mathbf{A}\cdot\mathbf{B}=\mathrm{tr}(\mathbf{A}^{\mathrm{T}}\mathbf{B})$ denotes the inner product between two second order tensors $\mathbf{A}$ and $\mathbf{B}$; and the symbol $\otimes$ denotes the tensor product.

2. Discussion of the previous model

In the previous one-dimensional model (Rubin et al., 1998), the elastic strain ε_{e} is determined by integrating an evolution equation of the form

$$\dot{\varepsilon}_{\mathrm{e}}=\dot{\varepsilon}-A_{\mathrm{i}}, \tag{1}$$

where $\dot{\varepsilon}$ is the total deformation rate and the inelastic strain rate A_{i} is specified by the constitutive equation

$$A_{\mathrm{i}}=D\varepsilon_{\mathrm{e}}, \tag{2a}$$

$$D=\frac{a+b|\dot{\varepsilon}|}{|\varepsilon_{\mathrm{e}}|}\exp\left[-\frac{1}{2}\left\{\frac{Z}{\sigma_{\mathrm{eff}}}\right\}^{2n}\right], \tag{2b}$$

$$\sigma_{\mathrm{eff}}=|\sigma|. \tag{2c}$$

Also, the stress σ is a nonlinear function of the elastic strain

$$\sigma=\sigma(\varepsilon_{\mathrm{e}}). \tag{3}$$

In these equations, the constant n controls the sharpness of the transition from primarily elastic to viscoplastic response and also controls rate sensitivity, Z is a measure of hardening, the constant a is important in relaxation tests ($|\dot{\varepsilon}|=0$), and the constant b dominates the inelastic response during loading. This model was used (Rubin et al., 1998) to obtain good agreement with the available experimental data.

In modeling metal plasticity, the term $b|\dot{\varepsilon}|$ in (2b) is usually set to zero so that the evolution equation (1) is explicitly rate dependent. However, in modeling SMAS and facial skin it was found that the term $b|\dot{\varepsilon}|$ is

significant during the loading cycles. More specifically, if a in (2b) vanishes, then the response of the evolution equation (1) becomes explicitly independent of time so that the physical condition (P6) will be satisfied. Consequently, by introducing the total deformation rate into the inelastic term A_i in (1), (2a), it is possible to satisfy the condition (P6) about the near rate independence of the hysteresis loops without the need for a large number of discrete relaxation times. Also, integration of the evolution equation (1) does not increase computer storage requirements as can occur in hereditary integral approaches to inelasticity.

During the experiments reported by Har-Shai et al. (1996) on recently excised facial skin, it was observed that liquid drops appeared on the tissue's outer surface as it was being loaded. In that paper it was speculated that the fluid transport associated with stressing the specimen was responsible for the apparent hardening phenomena. Thus, from the phenomenological point of view, this effect of fluid transport was modeled (Rubin et al., 1998) by proposing an evolution equation for the hardening variable Z of the form

$$\dot{Z} = mD\sigma_{\text{eff}}, \tag{4}$$

where m is a function that controls the rate of hardening and D is given by (2b).

Although Eqs. (1)–(4) provide a constitutive model that is consistent with the physical features (P1)–(P6) and produces reasonably good predictions of the experimental data, it neglects the physical phenomena that soft tissue in situ eventually recovers its original shape and its original stress–strain curves after it has been deformed and unloaded for sufficient time (neglecting aging effects). This presumably occurs as fluid is redistributed in the recovering tissue. Within the one-dimensional context, this phenomena can be modeled by including both an elastic component and recovery of hardening, which models recovery of fluid in the unloaded cells. In particular, a nonlinear version of a simple three element model with an elastic spring (the elastic component) can be used in parallel with a Maxwell element (the dissipative component) consisting of an elastic spring in series with a viscous dashpot. Specifically, the stress is assumed to be an additive function of the form

$$\sigma = \sigma_e(\varepsilon) + \sigma_d(\varepsilon_{de}), \qquad \sigma_{\text{eff}} = |\sigma_d|, \tag{5}$$

where σ_e is the stress response of the elastic component, which depends on total strain ε only, and σ_d is the stress response of the dissipative component, which depends on the elastic strain ε_{de} of the dissipative component. Moreover, the evolution equation (4) for hardening can be modified to take the form

$$\dot{Z} = mD\sigma_{\text{eff}} - R, \tag{6}$$

where the hardening recovery term R is a nonnegative function of the hardening variable that vanishes when Z vanishes

$$R = 0 \quad \text{for } Z = 0. \tag{7}$$

For appropriate constitutive equations, the unloaded tissue with zero total stress σ, will recover its original length ($\varepsilon = 0$) as ε_{de} and Z evolve towards zero.

3. General constitutive equations

Using standard notions in continuum mechanics, the position $\mathbf{X}$ of a material point in the fixed reference configuration is mapped to the position $\mathbf{x}$ in the present configuration at time t. Moreover, a material line element $d\mathbf{X}$ in the reference configuration is deformed into the material line element $d\mathbf{x}$ in the present configuration, such that

$$d\mathbf{x} = \mathbf{F}\, d\mathbf{X}, \tag{8a}$$

$$\mathbf{F} = \partial\mathbf{x}/\partial\mathbf{X}, \tag{8b}$$

$$J = \det \mathbf{F} > 0, \tag{8c}$$

$$\dot{\mathbf{F}} = \mathbf{L}\mathbf{F}, \tag{9a}$$

$$\mathbf{L} = \partial \mathbf{v}/\partial \mathbf{x}, \tag{9b}$$

$$\mathbf{D} = \tfrac{1}{2}(\mathbf{L} + \mathbf{L}^{\mathrm{T}}) = \mathbf{D}^{\mathrm{T}}, \tag{9c}$$

where $\mathbf{F}$ is the deformation gradient, J is the dilatation, $\mathbf{L}$ is the velocity gradient, $\mathbf{D}$ is the rate of deformation tensor, and a superposed $(\cdot)$ denotes material time differentiation holding $\mathbf{X}$ fixed. Also, within the context of the purely mechanical theory, it can be shown that the rate of dissipation $\mathscr{D}$ remains nonnegative

$$\mathscr{D} = \mathbf{T} \cdot \mathbf{D} - \rho \dot{\psi} \geqslant 0, \tag{10}$$

where $\mathbf{T}$ is the Cauchy stress, ρ is the current mass density and ψ is the strain energy function per unit mass.

The following analysis the tissue is considered to be a composite of elastic and dissipative components, and the affine assumption is used which considers each of these components to experience the same total strain. The elastic component depends on total deformation measures from the unstressed reference configuration and is assumed to be composed of a structure which responds to both total dilatation and distortion, as well as fiber constituents which respond to stretching. Also, the dissipative component is assumed to respond to distortional deformation.

In modeling the elastic component, it is recalled that for nonlinear isotropic elastic response the strain energy can be expressed as a function of the invariants of various deformation tensors. Here, use is made of the work of Flory (1961) to separate the total deformation tensor $\mathbf{B}$ into the dilatation J, which is a pure measure of volumetric deformation, and the symmetric tensor $\mathbf{B}'$, which is a pure measure of total distortional deformation, such that

$$\mathbf{B} = \mathbf{F}\mathbf{F}^{\mathrm{T}}, \tag{11a}$$

$$\mathbf{B}' = J^{-2/3}\mathbf{B}, \tag{11b}$$

$$\det(\mathbf{B}') = 1. \tag{11c}$$

Since $\mathbf{B}'$ is a unimodular tensor, it follows that it has only two independent nontrivial invariants which can be expressed as

$$\beta_1 = \mathbf{B}' \cdot \mathbf{I}, \quad \beta_2 = \mathbf{B}' \cdot \mathbf{B}'. \tag{12}$$

Also, using (9a) it can be shown that J and $\mathbf{B}'$ can, alternatively, be determined by integrating the evolution equations

$$\dot{J} = J\mathbf{D} \cdot \mathbf{I}, \tag{13a}$$

$$\dot{\mathbf{B}}' = \mathbf{L}\mathbf{B}' + \mathbf{B}'\mathbf{L}^{\mathrm{T}} - \tfrac{2}{3}(\mathbf{D} \cdot \mathbf{I})\mathbf{B}'. \tag{13b}$$

Thus, the material derivatives of β_1 and β_2 can be expressed in the forms

$$\dot{\beta}_1 = 2[\mathbf{B}' - \tfrac{1}{3}(\mathbf{B}' \cdot \mathbf{I})\mathbf{I}] \cdot \mathbf{D}, \tag{14a}$$

$$\dot{\beta}_2 = 4[\mathbf{B}'^2 - \tfrac{1}{3}(\mathbf{B}'^2 \cdot \mathbf{I})\mathbf{I}] \cdot \mathbf{D}. \tag{14b}$$

In modeling the dissipative component, it is recalled (Rubin, 1994a,b, 1996) that physically consistent constitutive equations for elastically anisotropic response of elastic–viscoplastic materials can be developed

using the work of Eckart (1948), Besseling (1968), and Leonov (1976). Specifically, for large deformations of elastically isotropic elastic–viscoplastic materials, it is convenient to introduce a symmetric unimodular tensor $\mathbf{B}'_{de}$, which is a pure measure of elastic distortional deformation associated with the dissipative component. This tensor is determined by integrating the evolution equation

$$\dot{\mathbf{B}}'_{de} = \mathbf{L}\mathbf{B}'_{de} + \mathbf{B}'_{de}\mathbf{L}^{T} - \tfrac{2}{3}(\mathbf{D}\cdot\mathbf{I})\mathbf{B}'_{de} - \Gamma\mathbf{A}_{d}, \tag{15a}$$

$$\det(\mathbf{B}'_{de}) = 1, \tag{15b}$$

$$\mathbf{A}_{d} = \mathbf{B}'_{de} - \left\{\frac{3}{\mathbf{B}'^{-1}_{de}\cdot\mathbf{I}}\right\}\mathbf{I}, \tag{15c}$$

$$\mathbf{A}_{d}\cdot\mathbf{B}'^{-1}_{de} = 0, \tag{15d}$$

where the rate of inelastic deformation is determined by the scalar function Γ and the symmetric tensor $\mathbf{A}_{d}$. The tensor $\mathbf{A}_{d}$ in (15d) is one of the simplest forms that causes elastic distortional deformation $\mathbf{B}'_{de}$ to remain a unimodular tensor (15b), and causes it to evolve towards the value $\mathbf{I}$. Moreover, since $\mathbf{B}'_{de}$ is a unimodular tensor it also has only two independent invariants

$$\alpha_{1} = \mathbf{B}'_{de}\cdot\mathbf{I}, \qquad \alpha_{2} = \mathbf{B}'_{de}\cdot\mathbf{B}'_{de}. \tag{16}$$

Furthermore, the material derivatives of α_1 and α_2 can be expressed in the forms

$$\dot{\alpha}_{1} = 2[\mathbf{B}'_{de} - \tfrac{1}{3}(\mathbf{B}'_{de}\cdot\mathbf{I})\mathbf{I}]\cdot\mathbf{D} - \Gamma\mathbf{A}_{d}\cdot\mathbf{I}, \tag{17a}$$

$$\dot{\alpha}_{2} = 4[\mathbf{B}'^{2}_{de} - \tfrac{1}{3}(\mathbf{B}'^{2}_{de}\cdot\mathbf{I})\mathbf{I}]\cdot\mathbf{D} - 2\Gamma\mathbf{A}_{d}\cdot\mathbf{B}'_{de}. \tag{17b}$$

Models of many soft tissues include explicit modeling of arrays of elastic fibers which have specific orientations in the tissues (e.g. Puso and Weiss, 1998; Holzapfel, 2001). In this regard, it is convenient to recall that with the help of (8a) and (9a), that the time rate of change of a material line element $d\mathbf{x}$ can be expressed in the form

$$d\dot{\mathbf{x}} = \mathbf{L}\,d\mathbf{x}. \tag{18}$$

Here, the anisotropic response of the tissue is modeled by N fiber components, each of which models the elastic response of an array of fibers oriented is a specific material direction. Moreover, in view of the affine assumption, arrays of fibers that have the same material orientation can be treated as a single fiber component which deforms like a line element. Specifically, let the unit vectors $\mathbf{M}_I$ ($I = 1, 2, \ldots, N$) characterize the orientations of these fiber components in the reference configuration, and let the vectors $\mathbf{m}_I$ characterize the orientations and stretches of these deformed fiber components in the present configuration, such that

$$\mathbf{m}_{I} = \mathbf{F}\mathbf{M}_{I}, \tag{19a}$$

$$\mathbf{M}_{I}\cdot\mathbf{M}_{I} = 1, \tag{19b}$$

$$\lambda_{I} = |\mathbf{m}_{I}|, \text{ (no sum on } I), \tag{19c}$$

where λ_I is the stretch of the line element $\mathbf{m}_I$, and the usual summation convention over repeated indices is suspended for capital indices. Thus, with the help of (18) it can be shown that alternatively, $\mathbf{m}_I$ can be determined by integrating the evolution equation

$$\dot{\mathbf{m}}_{I} = \mathbf{L}\mathbf{m}_{I}. \tag{20}$$

Furthermore, the material derivatives of λ_I can be expressed in the forms

$$\dot{\lambda}_I = \frac{1}{\lambda_I}(\mathbf{m}_I \otimes \mathbf{m}_I)\cdot\mathbf{D} \text{ (no sum on } I). \tag{21}$$

Assuming that the anisotropic response of tissue is due solely to the presence of specific arrays of fibers, it possible to model the nonlinear inelastic response of the tissue by taking the strain energy function ψ in the form

$$\psi = \psi(J, \beta_1, \beta_2, \alpha_1, \alpha_2, \lambda_I) \quad \text{for } I = 1, 2, \ldots, N. \tag{22}$$

Next, substituting (22) into (10), the resulting expression becomes a coefficient times $\mathbf{D}$ which includes the stress $\mathbf{T}$ and additional terms. Taking this coefficient of $\mathbf{D}$ equal to zero leads to the constitutive equation for stress in the form

$$\mathbf{T} = -p\mathbf{I} + \mathbf{T}', \qquad \mathbf{T}'\cdot\mathbf{I} = 0,$$

$$p = -\rho_0 \frac{\partial\psi}{\partial \mathrm{J}} - \sum_{I=1}^{N} \frac{1}{3}\rho_0 \frac{\partial\psi}{\partial\lambda_I} J^{-1}\lambda_I,$$

$$\begin{aligned}\mathbf{T}' = {} & 2\rho_0 \frac{\partial\psi}{\partial\beta_1} J^{-1}\left[\mathbf{B}' - \frac{1}{3}(\mathbf{B}'\cdot\mathbf{I})\mathbf{I}\right] + 4\rho_0 \frac{\partial\psi}{\partial\beta_2} J^{-1}\left[\mathbf{B}'^2 - \frac{1}{3}(\mathbf{B}'^2\cdot\mathbf{I})\mathbf{I}\right] + 2\rho_0 \frac{\partial\psi}{\partial\alpha_1} J^{-1}\left[\mathbf{B}'_{\mathrm{de}} - \frac{1}{3}(\mathbf{B}'_{\mathrm{de}}\cdot\mathbf{I})\mathbf{I}\right] \\ & + 4\rho_0 \frac{\partial\psi}{\partial\alpha_2} J^{-1}\left[\mathbf{B}'^2_{\mathrm{de}} - \frac{1}{3}(\mathbf{B}'^2_{\mathrm{de}}\cdot\mathbf{I})\mathbf{I}\right] + \sum_{I=1}^{N} \rho_0 \frac{\partial\psi}{\partial\lambda_I} J^{-1}\frac{1}{\lambda_I}\left[(\mathbf{m}_I\otimes\mathbf{m}_I) - \frac{1}{3}(\mathbf{m}_I\cdot\mathbf{m}_I)\mathbf{I}\right],\end{aligned} \tag{23}$$

and to the following expression for the dissipation (10)

$$\mathscr{D} = \rho_0 \frac{\partial\psi}{\partial\alpha_1} J^{-1}\Gamma\mathbf{A}_{\mathrm{d}}\cdot\mathbf{I} + 2\rho_0 \frac{\partial\psi}{\partial\alpha_2} J^{-1}\Gamma\mathbf{A}_{\mathrm{d}}\cdot\mathbf{B}'_{\mathrm{de}} \geqslant 0, \tag{24}$$

where ρ_0 is the reference value of the mass density, and use has been made of the conservation of mass in the form

$$\rho J = \rho_0. \tag{25}$$

The constitutive equations (23) are motivated by the necessary conditions required for the dissipation $\mathscr{D}$ to vanish whenever the material response is purely elastic ($\Gamma = 0$). However, in the present context, the functional form for Γ is left unspecified so that the Eqs. (23) and (24) are only sufficient conditions for the inequality (10) to be satisfied for all processes. These equations are hyperelastic in the sense that the stress is obtained by derivatives of a strain energy function, and it can be shown that they are properly invariant under superposed rigid body motions.

In (23) it can be seen that the dilatation J mainly influences the pressure p, the distortional deformation measures α_1, α_2, β_1, β_2 mainly influence the deviatoric stress $\mathbf{T}'$, and the stretches λ_I influence both p and $\mathbf{T}'$. Also, it is important to emphasize that in modeling soft tissue, the stress relaxation effects associated with the term $\Gamma\mathbf{A}_{\mathrm{d}}$ no longer model the effects of plasticity (as in the case of metals), but rather model the temporary internal microstructural changes associated with fluid flow and elastic distortion of cells.

4. Specific constitutive equations

The objective of this section is to develop specific simple constitutive equations to model the responses of SMAS and facial skin that are shown in Figs. 1 and 2. Also, the constitutive equations will be used to simulate response characteristics to loadings which demonstrate various physical features of the modeling. A number of polynomial and exponential functional forms for the strain energy ψ have been recorded in

Table 2 of Pioletti and Rakotomanana (2000). For simplicity, it will be assumed here that only one array of fibers is active and that the strain energy function takes the form

$$\rho_0\psi = \frac{\mu_0}{2q}[\exp(qg) - 1], \qquad g = g_1(J) + g_2(\beta_1) + g_3(\lambda_1) + g_4(\alpha_1), \tag{26}$$

where μ_0 is a material constant having the units of stress and q is a dimensionless constant that controls nonlinearity of the moduli for the different stress responses in the composite structure. Here, the function g separates into four parts, with g_1 characterizing the response to total dilatation, g_2 characterizing the response to total distortion, g_3 characterizing the response to stretching of the fiber component, and g_4 characterizing the response to distortional deformation of the dissipative component. In particular, these functions are specified by

$$g_1(J) = 2m_1[(J-1) - \ln(J)], \qquad g_2(\beta_1) = m_2(\beta_1 - 3),$$

$$g_3(\lambda_1) = \frac{m_3}{m_4}\langle\lambda_1 - 1\rangle^{2m_4}, \qquad g_4(\alpha_1) = \alpha_1 - 3, \tag{27}$$

where the material constants m_1, m_2, m_3 have been normalized relative to the constant μ_0.

Since material fibers are usually coiled, the elastic response to extension is highly nonlinear and the fiber component, which is modeled here, exhibits essentially zero stiffness to compression because it buckles (Puso and Weiss, 1998). For this reason, the McAuley brackets

$$\langle x\rangle = \tfrac{1}{2}(x + |x|), \tag{28}$$

have been used to eliminate the response to compression of the fiber component ($\lambda_1 < 1$). Furthermore, for the exponent $m_4 > 1$, the response of the fiber component will have zero stiffness initially in tension, which is consistent with its zero stiffness in compression.

It now follows from the results (23) that the constitutive equation for the stress associated with assumptions (26) and (27) becomes

$$\mathbf{T} = \mathbf{T}^{(1)} + \mathbf{T}^{(2)} + \mathbf{T}^{(3)} + \mathbf{T}^{(4)},$$

$$\mathbf{T}^{(1)} = -m_1\mu\left[\frac{1}{J} - 1\right]\mathbf{I}, \qquad \mathbf{T}^{(2)} = m_2\mu J^{-1}\mathbf{B}'',$$

$$\mathbf{T}^{(3)} = m_3\mu J^{-1}\frac{1}{\lambda_1}\langle\lambda_1 - 1\rangle^{2m_4-1}(\mathbf{m}_1 \otimes \mathbf{m}_1), \qquad \mathbf{T}^{(4)} = \mu J^{-1}\mathbf{B}''_{\mathrm{de}}, \tag{29}$$

where μ is the nonlinear shear modulus

$$\mu = \mu_0 \exp(qg), \tag{30}$$

and where the deviatoric tensors $\mathbf{B}''$ and $\mathbf{B}''_{\mathrm{de}}$ are defined by

$$\mathbf{B}'' = \mathbf{B}' - \tfrac{1}{3}(\mathbf{B}' \cdot \mathbf{I})\mathbf{I}, \qquad \mathbf{B}''_{\mathrm{de}} = \mathbf{B}'_{\mathrm{de}} - \tfrac{1}{3}(\mathbf{B}'_{\mathrm{de}} \cdot \mathbf{I})\mathbf{I}. \tag{31}$$

Also, it can be shown that the dissipation inequality (24) for these constitutive equations is automatically satisfied for all processes.

In attempting to simulate the response of SMAS and facial skin, it was first assumed that the strain energies associated with $\{J, \beta_1, \lambda_1, \alpha_1\}$ could each be specified by separate functions which may or may not have exponential terms. Specifically, the term associated with dissipation (α_1) was specified using an exponential form, whereas the other terms were of polynomial form. However, simulation of the resulting equations indicated that the stiffness of the response to dissipative distortional deformation increased so much, relative to say the response to volumetric deformation, that the total response became unphysical

with almost no distortional deformation and almost total volumetric deformation. Consequently, it was found necessary to include all terms in the same exponential function (26) so that the relative importance of the responses to volumetric and distortional deformations would remain the same even when the stiffness of each of these responses is nonlinear. This causes the response of the elastic component $\{\mathbf{T}^{(1)}, \mathbf{T}^{(2)}, \mathbf{T}^{(3)}\}$ to be coupled with that of the dissipative component $\{\mathbf{T}^{(4)}\}$ through the exponential term in the shear modulus (30).

The constitutive equation for the function Γ in the evolution Eq. (15a) for the elastic distortional deformation $\mathbf{B}'_{de}$ associated with the dissipative component, and for the evolution of a hardening-type variable, like that associated with (6), remains quite general. In this regard, it is well known that evolution equations of the type (15a) for viscoplastic response usually are stiff differential equations that can cause unphysical numerical instabilities. To eliminate this problem, special methods (Rubin, 1989; Rubin and Attia, 1996) have been developed, which are motivated by the radial return method, proposed by Wilkins (1964) for rate-independent plasticity.

To simplify the integration procedure, the functional form for Γ is written in terms of strain measures instead of stress measures. To this end, it is convenient to introduce a measure β_{de} of elastic distortional deformation associated with the dissipative component

$$\beta_{de} = \sqrt{\frac{3}{2}\mathbf{B}''_{de} \cdot \mathbf{B}''_{de}}, \tag{32}$$

which, in view of the expressions (29) and (31), can be seen to be related to the von Mises effective stress associated with the dissipative component. Moreover, in order for the resulting constitutive equations to satisfy the physical feature (P6), the functional form for Γ is proposed as

$$\Gamma = [\Gamma_1 + \Gamma_2 \dot{\varepsilon}] \exp\left[-\frac{1}{2}\left\{ \frac{\beta}{\beta_{de}} \right\}^{2n} \right], \tag{33}$$

where Γ_1 and Γ_2 and n are material constants. The effective total distortional deformation rate $\dot{\varepsilon}$ is defined by

$$\dot{\varepsilon} = \sqrt{\frac{2}{3}\mathbf{D}' \cdot \mathbf{D}'}, \qquad \mathbf{D}' = \mathbf{D} - \tfrac{1}{3}(\mathbf{D} \cdot \mathbf{I})\mathbf{I}, \tag{34}$$

and β is a hardening measure related to strain instead of stress. This theoretical form is a modified version of the unified constitutive equations developed by Bodner and Partom (1975) and Bodner (1987), and used by Rubin et al. (1998) to model soft tissue. In particular, it was found that a better match with the experimental data could be obtained by not dividing the expression in (33) by β_{de}, which would be similar to the form (2b). Also, it can be seen that when $\Gamma_2\,\dot{\varepsilon}$ dominates Γ_1 in (33), then the evolution equation (15a) becomes nearly rate independent, which is a necessary feature to be consistent with the physical observation (P6).

As previously discussed, the hardening variable β is used to model the effective hardening associated with fluid flow through the cells of the tissue. Here, β is determined by the evolution equation

$$\dot{\beta} = \left[\frac{r_1 r_3 + r_2 \dot{\varepsilon}}{r_3 + \dot{\varepsilon}} \right] \Gamma \beta_{de} - r_4 \beta^{r_5}, \tag{35}$$

where r_1–r_5 are additional positive material constants. For simplicity, the value of r_3 is taken to be very small so that coefficient of Γ is given by r_1 for stress relaxation tests with $\dot{\varepsilon} = 0$, and by r_2 for loading with $\dot{\varepsilon} > 0$. However, a more general function for Γ could be considered if more experimental data were available to determine the functional dependence on deformation rate. Also, the recovery rate is controlled

by the constants r_4 and r_5. In particular, for a stress relaxation test with constant deformation ($\mathbf{D} = 0$), the hardening variable β will eventually recover to zero, which causes $\mathbf{B}'_{de}$ to approach $\mathbf{I}$, so that the deviatoric stress $\mathbf{T}^{(4)}$ associated with the dissipative component relaxes to zero. Under these conditions the total stress is due solely to the response of the elastic component of the tissue.

In summary, the stress is determined by the constitutive equations (26), (27) and (29), which depend on the elastic constants

$$\{\mu_0, q\}, \tag{36a}$$

$$\{m_1, m_2, m_3, m_4\}. \tag{36b}$$

The evolution equation (15a) for the elastic distortional deformation $\mathbf{B}'_{de}$, associated with the dissipative component, depends on the material constants in (33)

$$\{\Gamma_1, \Gamma_2, n\}, \tag{37}$$

and the evolution equation (35) for the hardening variable β depends on the material constants

$$\{r_1, r_2\}, \tag{38a}$$

$$\{r_3, r_4, r_5\}. \tag{38b}$$

Moreover, initial conditions must be specified for the quantities

$$\{J, \mathbf{B}', \mathbf{B}'_{de}, \mathbf{m}_1, \beta\}, \tag{39}$$

in order to integrate the evolution equations (13a), (13b), (15a), (20) and (35), respectively. Once these equations have been integrated, the stretch λ_1 can be determined by the formula (19c). Furthermore, numerical integration algorithms for the evolution equations (15a) and (35) are briefly described in Appendix A.

5. Examples

In order to model the experiments on SMAS and facial skin shown in Figs. 1 and 2, it is necessary to consider the response to uniaxial stress. To this end, let $\mathbf{e}_i$ be a fixed orthonormal set of rectangular Cartesian base vectors and consider the motion specified by

$$x_1 = a_1 X_1, \qquad x_2 = a_2 X_2, \qquad x_3 = a_2 X_3, \tag{40}$$

where X_i and x_i are the components of $\mathbf{X}$ and $\mathbf{x}$, respectively, relative $\mathbf{e}_i$, and the stretches a_1 and a_2 are functions of time. For simplicity, the engineering strains ε_{11}, ε_{22} and ε_v are defined by

$$\varepsilon_{11} = a_1 - 1, \qquad \varepsilon_{22} = a_2 - 1, \qquad \varepsilon_v = J - 1, \tag{41}$$

with ε_{11} being the axial strain, ε_{22} being the lateral strain, and ε_v being the volumetric strain. In the following examples, the motion will be characterized by specifying $\dot{\varepsilon}_{11}$ to be piecewise constant, and the value of a_2 will be determined by iteration on the condition that the lateral component T_{22} of stress vanishes.

Next, it can be shown that for the motion (40), the velocity gradient $\mathbf{L}$ equals the rate of deformation tensor $\mathbf{D}$, which is a diagonal tensor. Consequently, with the assumption that in the initial configuration ($J = 1$, $\mathbf{B}' = \mathbf{I}$, $\mathbf{B}'_{de} = \mathbf{I}$, $\mathbf{m}_1 = \mathbf{e}_1$), the evolution equations (13a), (13b), (15a), and (20) can be integrated to deduce that

$$\mathbf{F} = a_1(\mathbf{e}_1 \otimes \mathbf{e}_1) + a_2(\mathbf{e}_2 \otimes \mathbf{e}_2 + \mathbf{e}_3 \otimes \mathbf{e}_3), \tag{42a}$$

$$J = a_1 a_2^2, \tag{42b}$$

$$\mathbf{B}' = \left[\frac{a_1}{a_2}\right]^{4/3}(\mathbf{e}_1 \otimes \mathbf{e}_1) + \left[\frac{a_2}{a_1}\right]^{2/3}(\mathbf{e}_2 \otimes \mathbf{e}_2 + \mathbf{e}_3 \otimes \mathbf{e}_3), \tag{42c}$$

$$\mathbf{m}_1 = a_1\mathbf{e}_1, \tag{42d}$$

$$\lambda_1 = a_1, \tag{42e}$$

$$\mathbf{B}'_{\mathrm{de}} = a_{\mathrm{d}}^2(\mathbf{e}_1 \otimes \mathbf{e}_1) + \frac{1}{a_{\mathrm{d}}}(\mathbf{e}_2 \otimes \mathbf{e}_2 + \mathbf{e}_3 \otimes \mathbf{e}_3), \tag{42f}$$

where the quantity a_{d} is determined by the evolution equation (15a) which reduces to

$$\frac{\dot{a}_{\mathrm{d}}}{a_{\mathrm{d}}} = \frac{2}{3}(D_{11} - D_{22}) - \Gamma\left[\frac{a_{\mathrm{d}}^3 - 1}{1 + 2a_{\mathrm{d}}^3}\right]. \tag{43}$$

It then follows from (29) and (42a)–(42f) that the nonzero components of the stresses relative to $\mathbf{e}_i$ are given by

$$T_{11}^{(1)} = T_{22}^{(1)} = T_{33}^{(1)} = -m_1\mu\left[\frac{1}{J} - 1\right],$$

$$T_{11}^{(2)} = m_2\mu J^{-1}\frac{2}{3}\left\{\left[\frac{a_1}{a_2}\right]^{4/3} - \left[\frac{a_2}{a_1}\right]^{2/3}\right\}, \qquad T_{22}^{(2)} = T_{33}^{(2)} = -\frac{1}{2}T_{11}^{(2)},$$

$$T_{11}^{(3)} = m_3\mu J^{-1}a_1\langle a_1 - 1\rangle^{2m_4-1}, \qquad T_{22}^{(3)} = T_{33}^{(3)} = 0,$$

$$T_{11}^{(4)} = \mu J^{-1}\frac{2}{3}\left\{a_{\mathrm{d}}^2 - \frac{1}{\mathrm{a_d}}\right\}, \qquad T_{22}^{(4)} = T_{33}^{(4)} = -\frac{1}{2}T_{11}^{(4)}. \tag{44}$$

Also, the nonsymmetric Piola–Kirchhoff stress $\boldsymbol{\Pi}$ is related to the Cauchy stress $\mathbf{T}$ by the formula

$$\boldsymbol{\Pi} = J\mathbf{T}\mathbf{F}^{-1}, \tag{45}$$

so that for this deformation, the component Π_{11} of the engineering stress it given by

$$\Pi_{11} = \left[\frac{\mathrm{J}}{\mathrm{a}_1}\right]T_{11} = a_2^2 T_{11}. \tag{46}$$

The experiments that were performed by Har-Shai et al. (1996) are not sufficient to determine the fourteen material constants (36a), (36b), (37), (38a) and (38b). Here, the seven material constants (36a), (37) and (38a) are determined by matching those experiments, and the remaining seven constants (36b) and (38b) are specified to exhibit specific physical features of the model. A procedure for determining the complete set of material constants from more extensive experimental data is discussed in Section 6.

Specifically, the constants (36b) and (38b) were specified by the following reasoning. It is assumed that the main response to volumetric deformation $\mathbf{T}^{(1)}$ can be characterized by the volumetric response of water. Therefore, it is convenient to specify the constant m_1 in terms of the bulk modulus k_1 of water, such that

$$k_1 = 2.2 \text{ GPa} \quad \text{with} \quad m_1 = \frac{k_1}{\mu_0}. \tag{47}$$

Furthermore, it is recalled that the constitutive equations in Rubin et al. (1998) successfully matched the experimental data in Figs. 1 and 2 even though they did not include any purely elastic component. Therefore, it is expected that the predominant response of these tissues is due to the elastic distortional

deformation $\mathbf{B}'_{de}$ associated with the dissipative component. For this reason the constants $\{m_2, m_3\}$ associated with the elastic distortional deformation and the fiber responses are taken to be small, and the value of m_4 was arbitrarily set equal to unity. The value of r_3 was set to be small enough to separate the effects of hardening during loading and relaxation tests. Also, the value r_5 was arbitrarily set equal to unity, and the value r_4 was set to be small enough not to cause significant recovery of hardening during the cycles of loading and stress relaxation, but was chosen to be large enough to cause significant recovery of hardening over a 24 h period.

Table 1 records the material constants for SMAS and facial skin which cause the theoretical predictions shown in Figs. 1 and 2 to be in good agreement with the experimental data. These material constants have been divided into two sets: those which are determined by the experimental data, and those which have been specified as described above.

The material response exhibited by the experimental data in Figs. 1 and 2 indicates that both SMAS and facial skin are highly nonlinear and dissipative in the range of strains and strain rates tested. This means that both elastic and dissipative effects are coupled so that the determination of material constants is complicated. The procedure used to determine the values given in Table 1 requires the user to perform a number of simulations in order to discover which regions of the material response are most affected by which parameters. Unfortunately, without additional experimental data this procedure does not lead to a unique set of material values.

In determining the material constants, the values of n in Eq. (33) were taken to be the same as those determined by Rubin et al. (1998), with the lower value of n (for facial skin) causing more dissipation (i.e. SMAS responds more elastically than skin). The initial slope of the loading curve in cycle 1 is mainly controlled by the constants $\{\mu_0, \Gamma_2\}$, and the nonlinearity of the unloading curves is mainly controlled by the constant q. The value of Γ_1 influences both the dissipation in cycle 3 and the rate of stress relaxation in Figs. 1(b) and 2(b). The constant r_1 controls the rate of hardening and the elastic range exhibited in the cycles 2 and 3, and the constant r_2 controls the shape of the relaxation curves.

The preceding procedure is based on the identification of the material constants with particular response characteristics under a specific set of loading conditions. However, the resulting equations with the determined material constants should be applicable for all loading histories consistent with the limitations of the general theory.

Table 1
Material constants for SMAS and facial skin

	SMAS	Facial skin
Material constants determined by available experimental data		
μ_0 (MPa)	2.0	0.9
q	25.0	36.0
Γ_1 (s^{-1})	0.01	0.009
Γ_2	20.0	10.0
n	1.0	0.5
r_1	5.0E + 3	30.0E + 3
r_2	6.0	15.0
Material constants set to exhibit specific physical features of the model		
k_1 (GPa)	2.2	2.2
m_2	0.01	0.01
m_3	0.1	0.1
m_4	1.0	1.0
r_3 (s^{-1})	1.0E − 10	1.0E − 10
r_4 (s^{-1})	1.0E − 4	1.0E − 4
r_5	1.0	1.0

Figs. 1 and 2 show that the theoretical predictions of these constitutive equations are in good agreement with the experimental data for SMAS and facial skin for both loading and relaxation cycles. The remaining Figs. 3–7 examine additional features of the response predicted by these equations. Figs. 3 and 4 show aspects of the response of SMAS during the loading cycle 1 shown in Fig. 1. Specifically, Fig. 3 exhibits two aspects of the exact nonlinear geometry used in the equations. Fig. 3(a) shows that the Cauchy stress T_{11} (stress per unit present area) is larger than the engineering stress Π_{11}. The response predicted by these constitutive equations is nearly isochoric with the volumetric strain ε_v remaining about 10^{-4}. Within the context of linearized geometry, isochoric deformation would cause the lateral strain to be equal to $(-\varepsilon_{11}/2)$ instead of the actual value ε_{22} predicted by the theory. Therefore, Fig. 3(b) shows the effect of nonlinear geometry on the lateral strain.

Fig. 4 shows the relative magnitudes of the four axial stress contributions. In particular, notice that for the specified constants, the value of the stress $T_{11}^{(2)}$, associated with purely elastic distortion, is nearly two orders of magnitude smaller than the total axial stress T_{11}; and the value of $T_{11}^{(3)}$, associated with the fiber

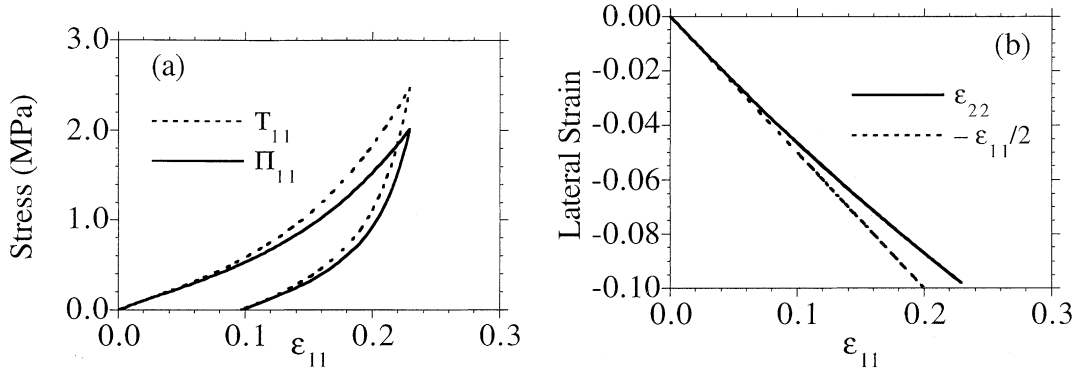

Fig. 3. Nonlinear geometrical effects exhibited in the response predicted during the loading cycle 1 for SMAS: (a) comparison of the Cauchy stress T_{11} with the engineering stress Π_{11}; (b) comparison of the lateral strain ε_{22} with that predicted by isochoric linear deformation $(-\varepsilon_{11}/2)$.

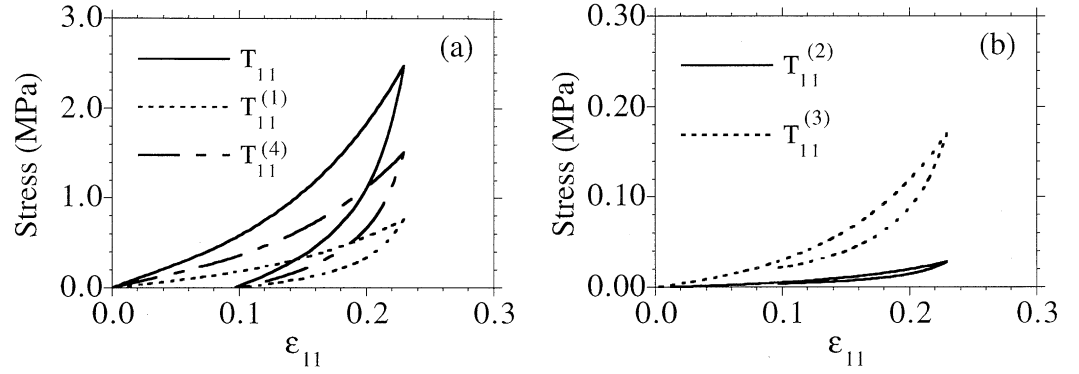

Fig. 4. Relative magnitudes of the various components of stress during the loading cycle 1 for SMAS. Comparison of: (a) the total axial stress T_{11} with the stress $T_{11}^{(1)}$ associated with volumetric deformation and the stress $T_{11}^{(4)}$ associated with dissipation; (b) the stress $T_{11}^{(2)}$ associated with purely elastic distortional deformation, and the stress $T_{11}^{(3)}$ associated with the fiber component.

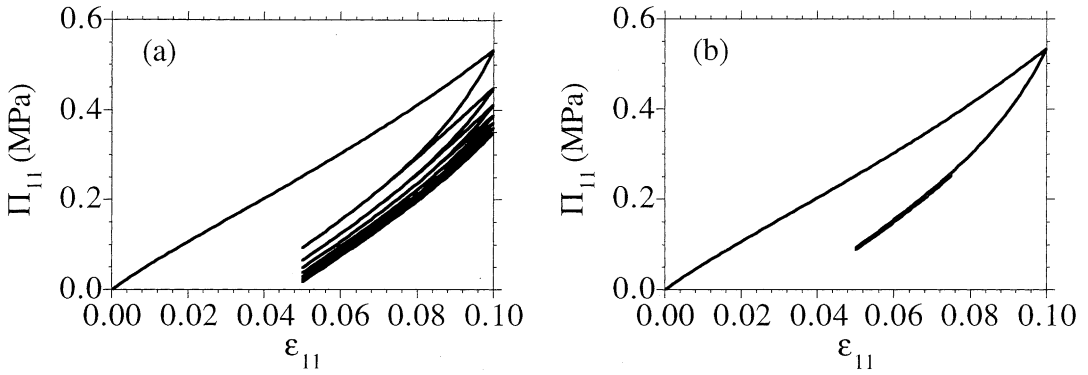

Fig. 5. Simulated conditioning of SMAS. Loading to $\varepsilon_{11} = 0.10$, unloading to $\varepsilon_{11} = 0.05$, followed by six cycles: (a) between $\varepsilon_{11} = 0.05$ and 0.10; and (b) between $\varepsilon_{11} = 0.05$ and 0.075. All loading and unloading occurs at the rate $\dot{\varepsilon}_{11} = \pm 2.0 \times 10^{-2}$ s^{-1}.

component, is about an order of magnitude smaller than T_{11}. The main contributions to the axial stress are the stress $T_{11}^{(1)}$, associated with volumetric deformation, and the stress $T_{11}^{(4)}$, associated with the dissipation component.

These figures demonstrate that the proposed model includes the physical features (P1)–(P3) of soft tissue which were described in Section 1. The additional physical features (P4) and (P5) can be observed in the simulations of Fig. 5. Specifically, in Fig. 5, the model for SMAS is loaded to $\varepsilon_{11} = 0.10$, unloaded to $\varepsilon_{11} = 0.05$ and then is subjected to six cycles of loading and unloading, all at the constant rate $\dot{\varepsilon}_{11} = \pm 2.0 \times 10^{-2}$ s^{-1}. In Fig. 5(a), the strain range of the additional cycles is between $\varepsilon_{11} = 0.05$ and 0.10, and dissipation occurs at a diminishing rate as the material continues to harden. In contrast, in Fig. 5(b), the strain range of the additional cycles is between $\varepsilon_{11} = 0.05$ and 0.075, and the response is nearly elastic.

Fig. 6 examines the effect of strain rate on SMAS. Specifically, it is recalled that the cycles 1, 2 and 3 in the experiments and in the simulations shown in Fig. 1(a) were conducted at different loading rates. The cycles shown in Fig. 6(a) and (b) are strain controlled and they use the same strain ranges as those in Fig. 1. However, all of the cycles shown in Fig. 6(a) are loaded at the constant rate $\dot{\varepsilon}_{11} = \pm 2.0 \times 10^{-2}$ s^{-1}, which is associated with cycle 1 in Fig. 1(a). Thus, the theoretical curve for cycle 1 in Fig. 6(a) is the same as that shown in Fig. 1(a). It can be observed that the response to cycle 2 in Fig. 6(a) is almost unaffected by the increase in strain rate by a factor of 4 compared with cycle 2 in Fig. 1(a), whereas the response to cycle 3 in Fig. 6(a) is slightly affected by the increase in strain rate by a factor of 20 compared with cycle 3 in Fig. 1(a). All of the cycles shown in Fig. 6(b) are loaded at the constant rate $\dot{\varepsilon}_{11} = \pm 2.0 \times 10^{-1}$ s^{-1}, which is 10 times higher than that used in Fig. 6(a). Comparison of the results in Fig. 6(b) with those in Fig. 6(a) demonstrates that when the strain rate is high enough, the material response is nearly rate insensitive, which is consistent with the physical feature (P6).

Fig. 7 shows the effect of recovery of hardening, which is associated with inward flow of fluid to the tissue. Specifically, in Fig. 7, SMAS is loaded to $\varepsilon_{11} = 0.1$ at a constant strain rate $\dot{\varepsilon}_{11} = 2.0 \times 10^{-2}$ s^{-1}, and then the strain is held constant and the material is allowed to relax. Fig. 7(a) shows the short-time response in which the stress relaxes and the hardening variable β continues to increase due to dissipation. Fig. 7(b) shows the long-time response in which the stress continues to relax as the hardening variable decreases due to recovery. In particular, it can be seen that the stress $T_{11}^{(4)}$ associated with the dissipative component decreases towards zero, whereas the stress $T_{11}^{(3)}$, associated with the fiber component, remains relatively constant.

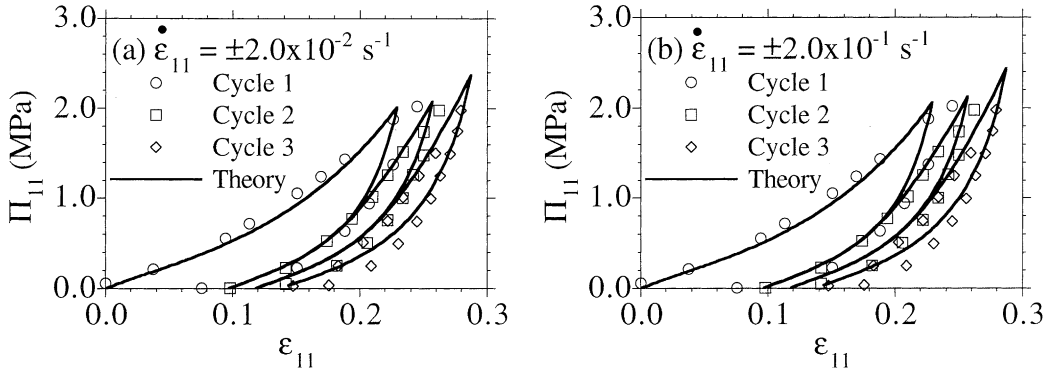

Fig. 6. Cyclic loading of SMAS showing near rate-insensitive response. All cycles are loaded at the same rate: (a) $\dot{\varepsilon}_{11} = \pm 2.0 \times 10^{-2}$ s^{-1}; (b) $\dot{\varepsilon}_{11} = \pm 2.0 \times 10^{-1}$ s^{-1}.

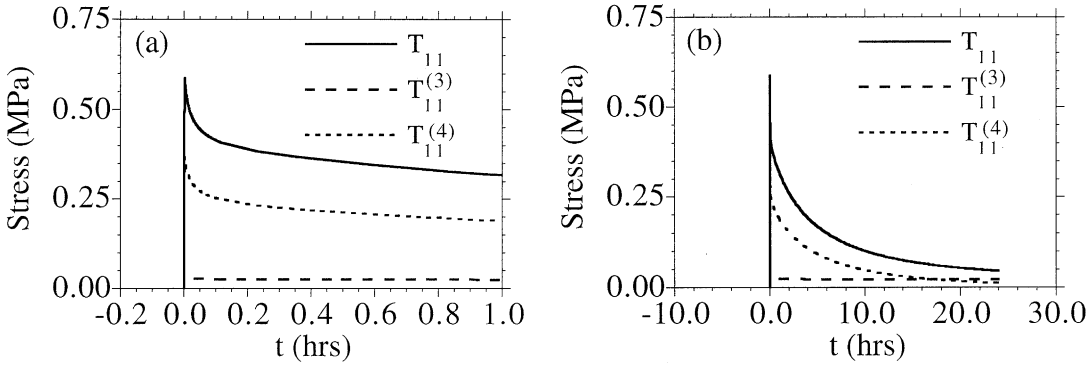

Fig. 7. Relaxation of SMAS. Loading to $\varepsilon_{11} = 0.1$ at a rate of $\dot{\varepsilon}_{11} = 2.0 \times 10^{-2}$ s^{-1} followed by stress relaxation: (a) over a short period, and (b) over a long period, with recovery of hardening.

6. Conclusions

In the previous sections, a set of three-dimensional constitutive equations has been proposed for modeling the nonlinear dissipative response of soft tissue. These equations model the tissue as a composite of elastic and dissipative components. The elastic component includes purely elastic response to dilatation, distortion and the stretch of material fiber components, and the dissipative component responds to distortional deformations. Specific functional forms have been proposed in Section 4, and material constants have been determined which yield good agreement with uniaxial stress experiments on SMAS and facial skin. The equations have been shown to exhibit the physical features (P1)–(P6) of soft tissue that have been described in Section 1. In particular, it is noted that, in contrast with standard viscoelastic models of tissues, the proposed constitutive equations include the total deformation rate in evolution equations in order to reproduce the observed physical feature (P6) that the hysteresis loops of most biological soft tissues are nearly independent of the strain rate (Fung, 1993).

As previously mentioned, the experiments of Har-Shai et al. (1996) are not sufficient to determine all of the material constants in the specific model of Section 4. However, an experimental procedure for determining the responses $\mathbf{T}^{(1)}$, $\mathbf{T}^{(2)}$, $\mathbf{T}^{(3)}$ of the elastic components and the response $\mathbf{T}^{(4)}$ of the dissipative component could be devised as follows:

The evolution Eq. (35) for the hardening variable β is phenomenological in nature and attempts to model the observed hardening due to loss of fluid during loading and dissipation, as well as recovery of hardening due to re-absorption of fluid. In particular, it follows from (15a)–(15d), (29), (33), and (35) that if the material is held at constant strain over a long time period, then both β and the stress $\mathbf{T}^{(4)}$, due to the dissipative component, approach zero. Consequently, the only remaining stresses are $\mathbf{T}^{(1)}$, $\mathbf{T}^{(2)}$ and $\mathbf{T}^{(3)}$ associated with the elastic components. This means that by performing experiments with different homogeneous total deformations, followed by long-time relaxation periods, it is possible to determine the constitutive equations for $\mathbf{T}^{(1)}$, $\mathbf{T}^{(2)}$ and $\mathbf{T}^{(3)}$. Specifically, since the fiber component (29) cannot support compression, the constants $\{m_1\mu_0, m_2\mu_0, q\}$ can be determined by matching uniaxial stress tests in directions perpendicular to the fiber component. Then, the constants $\{m_3\mu_0, m_4\}$ can be determined by matching uniaxial stress tests in the direction of the fiber component.

Once the material constants for purely elastic response have been determined, short-time loading and stress relaxation tests can be used to determine the dissipative material constants. Specifically, it is expected that $\{\mu_0\}$ can be determined by considering the Poisson effect in rapid uniaxial stress loading. Then, $\{\Gamma_2, n, r_2\}$ can be determined by matching the response to rapid loading–unloading–reloading cycles. Next, it is assumed that the recovery of hardening in (35) occurs over relatively long time periods, so that the short-time response in relaxation tests ($\dot{\varepsilon} = 0$) can be used to determine the constants $\{\Gamma_1\}$ in (33), and $\{r_1, r_3\}$ in (35). Then, long-time relaxation tests can be used to determine the constants $\{r_4, r_5\}$ in (35). In this regard, it should be noted that since comparison with a limited set of experiments is necessarily somewhat subjective, this general procedure may not lead to a unique set of material constants, which is typical when considering nonlinear time-dependent constitutive equations.

The equations proposed in this paper provide an alternative theoretical structure to the standard viscoelastic formulations that have been used to model soft tissue. The specific functional forms for the constitutive equations are rather simple and they model the main physical features of biological tissue. However, the functional forms for the evolutions equations can be modified to include more complicated physical features as additional experimental data becomes available.

Acknowledgements

The work of M.B. Rubin was partially supported by the Fund for Promotion of Research at Technion.

Appendix A. Numerical integration of the evolution equations

Following the numerical procedures developed in Rubin (1989), Rubin and Attia (1996), the evolution equation (15a) is integrated by assuming that $\mathbf{L}$ is constant over the time interval $\Delta t = t_2 - t_1$, and by considering an elastic trial solution $\mathbf{B}'^{*}_{\mathrm{de}}$ which is approximated by

$$\mathbf{B}'^{*}_{\mathrm{de}} = \mathbf{B}'_{\mathrm{de1}} + \Delta t[\mathbf{L}\mathbf{B}'_{\mathrm{de1}} + \mathbf{B}'_{\mathrm{de1}}\mathbf{L}^{\mathrm{T}} - \tfrac{2}{3}(\mathbf{D}\cdot\mathbf{I})\mathbf{B}'_{\mathrm{de1}}], \tag{A.1}$$

where for convenience, $\mathbf{B}'_{\mathrm{de1}}$ and $\mathbf{B}'_{\mathrm{de2}}$ denote the values of $\mathbf{B}'_{\mathrm{de}}$ at times t_1 and t_2, respectively. Also, the elastic trial values $\mathbf{B}''^{*}_{\mathrm{de}}$ and β^{*}_{de} are defined by

$$\mathbf{B}''^{*}_{\mathrm{de}} = \mathbf{B}'^{*}_{\mathrm{de}} - \frac{1}{3}(\mathbf{B}'^{*}_{\mathrm{de}}\cdot\mathbf{I})\mathbf{I}, \qquad \beta^{*}_{\mathrm{de}} = \sqrt{\frac{3}{2}\mathbf{B}''^{*}_{\mathrm{de}}\cdot\mathbf{B}''^{*}_{\mathrm{de}}}. \tag{A.2}$$

Then, the evolution Eq. (15a) can be integrated implicitly by taking

$$\mathbf{B}'_{\mathrm{de2}} = \mathbf{B}'^{*}_{\mathrm{de}} - \Delta t\,\Gamma(t_2)\mathbf{A}_{\mathrm{d}}(t_2). \tag{A.3}$$

Consequently, with the help of (15c), the deviatoric part of (A.3) yields

$$[1+\Delta t\,\Gamma(t_2)]\mathbf{B}''_{\mathrm{de}2}=\mathbf{B}''^{*}_{\mathrm{de}}. \tag{A.4}$$

Now, the notion of radial return suggests that

$$\mathbf{B}''_{\mathrm{de}2}=\lambda\mathbf{B}''^{*}_{\mathrm{de}},\quad \beta_{\mathrm{e}2}=\beta_{\mathrm{de}}(t_2)=\lambda\beta^{*}_{\mathrm{de}},\qquad 0\leqslant\lambda\leqslant 1, \tag{A.5}$$

where λ is a scalar (not to be confused with the stretch of a material fiber component) that is determined by the equation

$$1=[1+\Delta t\,\Gamma(t_2)]\lambda. \tag{A.6}$$

Thus, it follows that λ equals unity for elastic response ($\Gamma=0$) and is less than unity for dissipative response. Moreover, assuming that the hardening variable β does not change too rapidly during a single time step, the value of λ can be determined by iteration until (A.6) is satisfied with $\Gamma(t_2)$ given by

$$\Gamma(t_2)=[\Gamma_1+\Gamma_2\dot{\varepsilon}]\exp\left[-\frac{1}{2}\left\{\frac{\beta(t_1)}{\lambda\beta^{*}_{\mathrm{de}}}\right\}^{2n}\right], \tag{A.7}$$

where $\beta(t_1)$ is the value of β associated with the beginning of the time step. Once λ has been determined, $\mathbf{B}''_{\mathrm{de}2}$ and $\beta_{\mathrm{e}2}$ are given by (A.5). Also, the value of distortional deformation $\mathbf{B}'_{\mathrm{e}}(t_2)$ at the end of the time step can be written in the form

$$\mathbf{B}'_{\mathrm{de}}(t_2)=\mathbf{B}''_{\mathrm{de}2}+\tfrac{1}{3}\beta_1(t_2)\mathbf{I}, \tag{A.8}$$

where the value of the invariant $\beta_1(t_2)$ is determined by a cubic equation which requires $\mathbf{B}'_{\mathrm{de}}$ to be a unimodular tensor (Rubin and Attia, 1996).

For the specific deformation considered in the examples in Section 4, the elastic trial value a^{*}_{d} associated with integrating (43), with Γ vanishing, can be expressed in the form

$$a^{*}_{\mathrm{d}}=a_{\mathrm{d}}(t_1)\exp\left[\tfrac{2}{3}\Delta t(D_{11}-D_{22})\right]. \tag{A.9}$$

Then, the elastic trial value $\mathbf{B}'^{*}_{\mathrm{de}}$ becomes

$$\mathbf{B}'^{*}_{\mathrm{de}}=a^{*2}_{\mathrm{d}}(\mathbf{e}_1\otimes\mathbf{e}_1)+\frac{1}{a^{*}_{\mathrm{d}}}(\mathbf{e}_2\otimes\mathbf{e}_2+\mathbf{e}_3\otimes\mathbf{e}_3). \tag{A.10}$$

Also, the values of D_{11} and D_{22} are approximated by

$$D_{11}=\frac{\dot{\varepsilon}_{11}}{a(t_1)+\frac{\Delta t\,\dot{\varepsilon}_{11}}{2}},\qquad D_{22}=\frac{\dot{\varepsilon}_{22}}{b(t_1)+\frac{\Delta t\,\varepsilon_{22}}{2}}. \tag{A.11}$$

Finally, simple Euler integration is used to determine the value of hardening associated with the evolution equation (35)

$$\beta(t_2)=\beta(t_1)+\Delta t\left[\left\{\frac{r_1r_3+r_2\dot{\varepsilon}}{r_3+\dot{\varepsilon}}\right\}\Gamma(t_2)\beta_{\mathrm{de}}(t_1)-r_4\{\beta(t_1)\}^{r_5}\right]. \tag{A.12}$$

References

Besseling, J.F., 1968. A thermodynamic approach to rheology. In: Parkus, H., Sedov, L.I. (Eds.), Proc. of the IUTAM Symposium on Irreversible Aspects of Continuum Mechanics and Transfer of Physical Characteristics in Moving Fluids, Vienna, 1966. Springer-Verlag, Wein, pp. 16–53.

Bodner, S.R., 1987. Review of a unified elastic–viscoplastic theory. In: Miller, A.K. (Ed.), Unified Constitutive Equations for Creep and Plasticity. Elsevier Applied Science Publications, London, pp. 273–301.

Bodner, S.R., Partom, Y., 1975. Constitutive equations for elastic–viscoplastic strain-hardening materials. ASME J. Appl. Mech. 42, 385–389.

Choung, C.J., Fung, Y.C., 1986. Residual stress in arteries. In: Frontiers in Biomechanics. Springer-Verlag, New York, pp. 117–179.

Eckart, C., 1948. The thermodynamics of irreversible processes IV. The theory of elasticity and anelasticity. Phys. Rev. 73, 373–382.

Flory, P., 1961. Thermodynamic relations for high elastic materials. Trans. Faraday Soc. 57, 829–838.

Fung, Y.C., 1993. Biomechanics, Mechanical Properties of Living Tissues, second ed. Springer-Verlag, New York.

Har-Shai, Y., Bodner, S.R., Egozy-Golan, D., Lindenbaum, E.S., Ben-Izhak, O., Mitz, V., Hirshowitz, B., 1996. Mechanical properties and microstructure of the superficial musculoaponeurotic system. Plastic Reconstruct. Surgery 98, 59–70.

Holzapfel, G.A., 2001. Biomechanics of soft tissue. In: Lemaitre, J. (Ed.), Handbook of Materials Behavior Models, vol. III, Multiphysics Behaviors. Academic Press, San Diego, pp. 1057–1071.

Horowitz, A., Sheinman, I., Lanir, Y., 1988. Nonlinear incompressible finite element for simulating loading of cardiac tissue—part II: three-dimensional formulation for thick ventricular wall segments. ASME J. Biomech. Eng. 110, 62–68.

Humphrey, J.D., Yin, F.C.P., 1987. On constitutive relations and finite deformations of passive cardiac tissue. ASME J. Biomech. Eng. 109, 298–304.

Humphrey, J.D., Strumph, R.K., Yin, F.C.P., 1990. Determination of a constitutive relation for passive myocardium. ASME J. Biomech. Eng. 112, 333–339.

Huyghe, J.M.R.J., Janssen, J.D., 1999. Thermo-chemo-electro-mechanical formulation of saturated charged porous media. Transport Eng. 34, 129–141.

Leonov, A.I., 1976. Nonequilibrium thermodynamics and rheology of viscoelastic polymer media. Rheologica Acta 15, 85–98.

Neubert, H.K.P., 1963. A simple model representing internal damping in solid materials. Aeronaut. Quarterly 14, 187–210.

Pioletti, D.P., Rakotomanana, L.R., 2000. Non-linear viscoelastic laws for soft biological tissues. Eur. J. Mech. A/Solids 19, 749–759.

Puso, M.A., Weiss, J.A., 1998. Finite element implementation of anisotropic quasi-linear viscoelasticity using a discrete spectrum approximation. ASME J. Biomech. Eng. 120, 62–70.

Rubin, M.B., 1989. A time integration procedure for plastic deformation in elastic–viscoplastic metals. J. Appl. Math. Phys. (ZAMP) 40, 846–871.

Rubin, M.B., 1994a. Plasticity theory formulated in terms of physically based microstructural variables—part I: theory. Int. J. Solids Struct. 31, 2615–2634.

Rubin, M.B., 1994b. Plasticity theory formulated in terms of physically based microstructural variables—part II: examples. Int. J. Solids Struct. 31, 2635–2652.

Rubin, M.B., 1996. On the treatment of elastic deformation in finite elastic–viscoplastic theory. Int. J. Plasticity 12, 951–965.

Rubin, M.B., Attia, A., 1996. Calculation of hyperelastic response of finitely deformed elastic–viscoplastic materials. Int. J. Numer. Meth. Eng. 39, 309–320.

Rubin, M.B., Bodner, S.R., Binur, N.S., 1998. An elastic–viscoplastic model for excised facial tissues. ASME J. Biomech. Eng. 120, 686–689.

Vankan, W.J., Huyghe, J.M.R.J., Drost, M.R., Janssen, J.D., Huson, A., 1997. A finite element mixture model for hierarchical porous media. Int. J. Numer. Meth. Eng. 40, 193–210.

Wilkins, M.L., 1964. Calculation of elastic–plastic flow. In: Methods in Computational Physics, vol. 3. Academic press, New York, pp. 211–263.